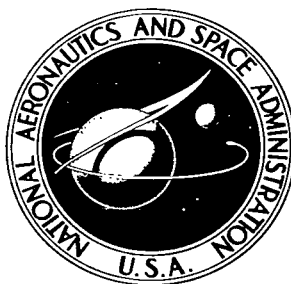


NASA TECHNICAL NOTE



NASA TN D-4070

c. 1

10/11/67
AUG 1967
KIRTLAND AFB



NASA TN D-4070

EFFECTS OF FLUID PROPERTIES AND GRAVITY LEVEL ON BOILING IN THE DISCRETE BUBBLE REGION

by Thomas H. Cochran and John C. Aydelott

Lewis Research Center

Cleveland, Ohio



0130959

NASA TN D-4070

EFFECTS OF FLUID PROPERTIES AND GRAVITY LEVEL ON BOILING
IN THE DISCRETE BUBBLE REGION

By Thomas H. Cochran and John C. Aydelott

Lewis Research Center
Cleveland, Ohio

NATIONAL AERONAUTICS AND SPACE ADMINISTRATION

For sale by the Clearinghouse for Federal Scientific and Technical Information
Springfield, Virginia 22151 - CFSTI price \$3.00

EFFECTS OF FLUID PROPERTIES AND GRAVITY LEVEL ON BOILING IN THE DISCRETE BUBBLE REGION

by Thomas H. Cochran and John C. Aydelott

Lewis Research Center

SUMMARY

The effects on boiling of changes in fluid properties and gravity level were investigated for liquids of high viscosity (a sucrose solution) and low surface tension (an ethanol-water solution) in relation to water. The zero-gravity data were obtained by allowing the experiment package to free fall in a 2.25-second drop tower, which permitted the attainment of less than 10^{-5} times Earth gravity. Data taken from high-speed motion pictures indicate that viscous effects were negligible during the growth of bubbles. However, in zero gravity, the viscous effects were important near bubble separation for the sucrose solution. Bubbles generated in the ethanol-water solution had similar maximum radii and lifetime characteristics in normal and zero gravities.

INTRODUCTION

The development of vehicles for space exploration has prompted investigation of the effect of gravity level on the transfer of heat to fluids. A particular area of interest is the storage of cryogenic liquids in closed containers over long periods of time, as would occur on a coasting space flight. Under such conditions, energy input from solar radiation will cause the tank pressure to increase, and as a result, the liquid may become subcooled (ref. 1). Consequently, a heat-transfer phenomenon of importance in reduced gravity is the subcooled nucleate boiling process.

In a recent study (ref. 2), the authors investigated the effect of subcooling and gravity level on the boiling characteristics and bubble dynamics of water vapor generated on a flat horizontal surface. The results indicate the gravity-independent nature of boiling at high subcooling conditions and the importance of a newly defined pressure force on bubble dynamics.

The present work is concerned with the effect of liquid properties and gravity level

on the dynamics of bubbles formed on a flat horizontal surface. The liquids investigated were a 60 percent by weight sugar-water solution, sucrose, and a 10 percent by volume ethanol-water solution. In relation to water, the sucrose solution had a greater viscosity, while the ethanol-water solution was characterized by a reduced surface tension. High-speed motion pictures were taken at subcoolings of approximately 6° , 15° , and 21° F (3.34° , 8.34° , and 11.67° C), in both normal gravity and in an environment of less than 10^{-5} times normal gravity. The heat flux selected was in the range defined in normal gravity as the discrete bubble region (ref. 3). For such heat fluxes in normal gravity, the bubbles generally grow singularly on the heated surface, and the heat-transfer mechanism is dependent on the disturbance in the liquid caused by the growth and departure of the bubbles.

The photographic data were analyzed by measuring the bubble growth characteristics and calculating the forces acting on the bubbles during their growth.

APPARATUS, EXPERIMENTAL PROCEDURE, AND DATA REDUCTION

Because the apparatus, experimental procedure, and data reduction procedures are presented in detail in reference 2, only a brief description of them is given herein.

The zero-gravity data were obtained in a drop tower by allowing the experiment package to free fall unguided for 85 feet (25.91 m). A gravity level of less than 10^{-5} times Earth gravity (termed zero gravity in this report) resulted from the package falling in a protective air-drag shield. Deceleration occurred after 2.25 seconds when wooden spikes on the drag shield embedded in a box of sand. The experiment package contained a boiling apparatus, camera and lighting equipment, power supplies, and associated controls. Within the boiling apparatus, which is shown in figure 1, were the primary heater (a Chromel strip 0.5 in. wide by 0.005 in. thick by 0.5 in. long (1.27 by 0.0127 by 1.27 cm)), a secondary heater which was used to raise the bulk of the liquid to the saturation temperature, a thermistor to monitor the bulk temperature, and a thermocouple attached to the underside of the heater. The 16-millimeter motion-picture camera provided a filming rate of approximately 6500 pictures per second.

Prior to a data run the glassware was cleaned and the primary heater was polished and rinsed with ethanol. The test liquids were deaerated by boiling the sucrose solution for approximately 1 hour and the ethanol-water solution for approximately 20 minutes. The ethanol-water solution was boiled for a shorter time to maintain the alcohol concentration as near 10 percent by volume as possible. After filling the boiler and raising the apparatus to the top of the drop tower, the liquid was heated with the secondary heater to approximately the saturation temperature. Power to this heater was removed, and the

primary heater was turned on and set at a power level that initiated boiling. Because the heat input by the primary heater was not sufficient to maintain saturation conditions, the liquid bulk became subcooled. The power level to the heater was then increased to the desired level and the package was dropped. Motion pictures were taken during the last 1.25 seconds of zero-gravity time. Normal-gravity testing was the same as that just described with the addition that the thermocouple was monitored with a millivolt potentiometer.

The bubbles recorded on the film were viewed and measured on a motion analyzer that magnified the image eight times. A statistical analysis involved the recording of bubble lifetime and maximum radius for as many as 15 bubbles at each test condition. As a result of this study, an average bubble at each test condition was selected for a force analysis.

The forces calculated (ref. 2) were

the buoyancy force

$$F_B = (V - V_b)\rho_l \frac{g}{g_c} \quad (1)$$

the surface-tension force

$$F_{sy} = \sigma_S \pi D_b \sin \varphi \quad (2)$$

the pressure force

$$F_P = \frac{1}{2} \left(\frac{\pi D_b^2}{R_t} \right) \sigma_{sat} \quad (3)$$

the drag force

$$F_{dr} = 12\mu_l R_{max} \left(\frac{dy}{dt} \right) \quad (4)$$

and the dynamic force

$$F_{dy} = \frac{\rho_v}{g_c} \left(\frac{dV}{dt} \frac{dy}{dt} + V \frac{d^2y}{dt^2} \right) + F_{dr} + F_{sy} - F_B - F_P \quad (5)$$

(All symbols are defined in appendix A.) A slightly different approach in determining the viscous effects on the bubble than that taken in reference 2 was applied and is outlined in the section Effect of Viscosity on Bubble Dynamics. Force histories (plots of force

against time) were prepared for each bubble so that the effect of fluid property changes could be studied.

DETERMINATION OF FLUID PROPERTIES

A study was made to determine the pertinent physical properties of the test liquids. Surface tension as a function of temperature was calculated for the different liquids and is presented in figure 2(a). The method of calculation is given in appendix B. Changes in viscosity with temperature were described in reference 4 for the sucrose solution and in reference 5 for water. Values for the ethanol-water solution (fig. 2(b)) had to be obtained from measurements made with a rolling-ball-type viscosimeter. The specific gravity of water was taken from reference 6 and that of the ethanol-water solution was calculated from the values for water and pure ethanol (refs. 6 and 7). The specific gravity of the sucrose solution was obtained from both the literature (ref. 8) and experimental data, as shown in figure 2(c).

RESULTS AND DISCUSSION

Boiling Characteristics

General. - The temperature and heat-flux measurements taken during the normal and zero-gravity tests are presented in table I. Approximate saturation temperatures for use in computing the subcoolings were obtained by recording the highest bulk temperature attained after boiling for 5 to 10 minutes at a full boil. As in reference 2, average surface temperatures were tabulated because of the fluctuations.

Sucrose solution. - The sucrose-solution films indicate that only continuous growth bubbles were generated at all test conditions. Coalescence was evident in all the films and occurred most frequently at low subcooling in zero gravity. However, coalescence never became as frequent as it did under comparable conditions with water because the population density of the bubbles in the sucrose solution was much smaller. In reference 1, two types of coalescence are described. The first type, which occurred at low subcooling in normal and zero gravities, is characterized by two or more adjacent bubbles combining on the surface to form an irregular vapor mass. The second type was seen only at low subcooling in zero gravity and was caused by the bubbles moving so slowly away from the surface after separation that subsequent bubbles forming on the heater surface were eventually absorbed into the rising vapor mass. Both of these types of coalescence were observed in the sucrose solution along with a third type, which was present in both normal and zero gravities. In this third type of coalescence, an initial

bubble formed on the surface and departed; just as this bubble separated, a second one was generated from the same nucleation site. Since the growth rate of bubbles is a maximum early in their lifetime (ref. 2) and is relatively large for the sucrose solution (ref. 9), the second bubble rapidly merged with the underside of the initial bubble, and an irregular vapor mass was formed. This process is shown, in a series of photographs, in figure 3. Therefore, the primary difference between the second and third types of coalescence is that the cause of the former is the slowness of the bubbles caused by the absence of gravity as they depart from the vicinity of the heating surface, while the cause of the latter is the high initial growth rate of secondary bubbles.

The results of the sucrose-solution statistical study indicate the same general trends with subcooling as for water. As shown in figure 4, the average maximum radii and lifetimes of both liquids became smaller in both gravity levels as subcooling was increased. The effect of gravity level for the sucrose solution, however, was quite different from that for water. The sucrose bubbles were, on the average, larger in zero gravity than in normal gravity, but the considerable increase in size at low subcooling with a reduction in gravity evident in the water data did not occur for sucrose. This effect has also been noted by Keshock and Siegel (ref. 9). Examination of average bubble lifetime shows a considerable increase at zero gravity compared with normal gravity, particularly at low subcooling. Therefore, in a sucrose solution, boiling is gravity dependent close to saturation conditions, as evidenced by the fact that the bubbles remain on the heater surface approximately twice as long in zero gravity as in normal gravity.

Ethanol-water solution. - The ethanol-water films revealed that the majority of the bubbles generated under all test conditions were of the continuous growth type. Occasional coalescence of adjacent bubbles occurred at low subcooling in normal gravity but little coalescence was evident at high subcooling in either normal or zero gravities. More coalescence was noticeable at low subcooling in zero gravity; however, it never became frequent enough to dominate the phenomenon. Also some oscillators (alternately growing and collapsing bubbles) were observed in the low-subcooling zero-gravity test. Frequency of bubble generation was greater with the ethanol-water solution than with either sucrose or water. The bubble frequency became so great at one site it appeared that more than one bubble was being generated at the same time. Keshock and Siegel reported this phenomenon in reference 9 as a dominant characteristic of boiling pure ethanol. The necking down and large contact angles reported in reference 2 as characteristic of water bubbles at separation were not observed for bubbles generated in the ethanol-water solution.

The statistical study of the ethanol-water solution revealed the usual changes in bubble average maximum radius and lifetime with subcooling, as shown in figure 4. However, comparison of the normal and zero-gravity data indicates little difference for either the average maximum radius or average lifetime curves. In fact, the difference

between the normal and zero-gravity results can be attributed to statistical scatter. No importance should be attached to the apparent reversal in the curves as compared with those for the water data. Care should be taken at this point not to assume gravity independence. Although similarity at both normal and zero gravities is certainly a necessary condition for gravity independence, it is not sufficient. In addition, the forces acting on the bubbles must be investigated to ascertain the importance of gravity.

Effect of Viscosity on Bubble Dynamics

In reference 2, the viscous effects on a bubble were accounted for by a drag force, by assuming that liquid flowed around the bubble. After bubble profiles were observed (see fig. 5), it was concluded that this assumption was invalid during the growth of a bubble and that the liquid flow was more closely approximated by a source flow. Therefore, viscous effects in the early portion of bubble lifetime can be determined from the equations governing liquid motion. For a Newtonian, incompressible liquid with constant viscosity, and when body forces are neglected the pertinent equations are

Continuity:

$$\frac{\partial v_r}{\partial r} + \frac{1}{r} \frac{\partial v_\theta}{\partial \theta} + \frac{v_r}{r} = 0 \quad (6)$$

Navier-Stokes:

$$\rho_l \left(\frac{\partial v_r}{\partial t} + v_r \frac{\partial v_r}{\partial r} + \frac{v_\theta}{r} \frac{\partial v_r}{\partial \theta} - \frac{v_\theta^2}{r} \right) = - \frac{\partial P}{\partial r} + \mu_l \left(\frac{\partial^2 v_r}{\partial r^2} + \frac{1}{r^2} \frac{\partial^2 v_r}{\partial \theta^2} + \frac{1}{r} \frac{\partial v_r}{\partial \theta} - \frac{2}{r^2} \frac{\partial v_\theta}{\partial \theta} - \frac{v_r}{r^2} \right) \quad (7)$$

where r is measured radially away from the nucleation site and θ is the counterclockwise angular displacement of the r vector from the heater surface.

If it is assumed that $v_\theta \cong 0$, these equations reduce to

Continuity:

$$\frac{\partial v_r}{\partial r} + \frac{v_r}{r} = 0 \quad (8)$$

Navier-Stokes:

$$\rho_l \left(\frac{\partial \mathbf{v}_r}{\partial t} + \mathbf{v}_r \frac{\partial \mathbf{v}_r}{\partial r} \right) = - \frac{\partial P}{\partial r} + \mu_l \left(\frac{\partial^2 \mathbf{v}_r}{\partial r^2} + \frac{1}{r^2} \frac{\partial^2 \mathbf{v}_r}{\partial \theta^2} + \frac{1}{r} \frac{\partial \mathbf{v}_r}{\partial r} - \frac{\mathbf{v}_r}{r^2} \right) \quad (9)$$

Substituting equation (8) into equation (9) results in further reduction to

$$\rho_l \left(\frac{\partial \mathbf{v}_r}{\partial t} + \mathbf{v}_r \frac{\partial \mathbf{v}_r}{\partial r} \right) = - \frac{\partial P}{\partial r} + \mu_l \left(\frac{1}{r^2} \frac{\partial^2 \mathbf{v}_r}{\partial \theta^2} \right) \quad (10)$$

It is not necessary to solve these equations to ascertain the importance of viscosity. Instead, it can be obtained by comparing the magnitude of the viscous and liquid inertia terms in equation (10). This comparison was made for a sucrose bubble generated at 5° F (2.78° C) subcooling in normal gravity. The terms were evaluated for four values of θ from 10° to 90° and for eight time increments during the growth of the bubble. A representative cross section of the results, presented in table II, indicates that the absolute magnitude of the viscous terms is always much less than that of the liquid inertia terms. Therefore, the viscous effects in a direction perpendicular to the heater surface can be neglected during the growth of a bubble on a surface.

For the collapse portion of bubble lifetime, it was apparent (fig. 5) that there was some evidence of liquid flow around the bubble. Therefore, for this portion of the bubble history, the viscous effects were approximated by the drag formula presented in equation (4). Force histories for the sucrose bubbles at 15° F (8.34° C) subcooling in normal and zero gravities are presented in figure 6. It is evident that the bubbles were gravity dependent as indicated by (1) the large buoyant force in normal gravity and (2) the dissimilarity in the force histories between normal and zero gravity conditions. The normal gravity plot shows that the drag force always assumed a minor role in determining bubble motion. However, in zero gravity near separation, because of the absence of buoyancy and the reduction in the absolute value of the dynamic force, the drag force is comparable to the other forces and is important in determining the resultant motion of the bubble.

Effect of Surface Tension on Bubble Dynamics

The statistical analysis (fig. 4) shows that, for the ethanol-water solution, similar bubble maximum-radii and lifetime characteristics were obtained in normal and zero gravities at comparable subcoolings. At high subcooling, this result is readily explained by the small role of buoyancy in normal gravity and the similar force histories, as shown

in figure 7. However, investigation of the force histories for low subcooling (fig. 8) reveals a great difference between the normal and zero-gravity plots. Because of this basic change in the bubble dynamics, an alteration in the growth characteristics (average maximum radius or lifetime) of the bubbles could be expected. However, since the statistical data showed that these characteristics were not affected by gravity, it is apparent that a change or changes took place in zero gravity in addition to the effective absence of gravity.

Comparison of the ethanol-water force histories with those for water (a typical history is shown in fig. 9) indicates that for a bubble in the ethanol-water solution the pressure force remains relatively large over the lifetime, while for a bubble in water it decreases rapidly from a large value near inception. The cause for this phenomenon is related to the shape of the bubbles. Siegel, in reference 10, suggests that for a bubble to be spherical the absolute magnitude of the ratio of the pressure force to the surface-tension force is 1. Therefore, a measure of the distortion of a bubble can be obtained from the deviation of this ratio from 1. As shown in figure 10, where the distortion ratio is plotted as a function of dimensionless time (the ratio of real time to lifetime), the ethanol-water bubbles were, in general, more spherical than water bubbles. Further, at low subcooling the ethanol-water bubbles in zero gravity were more spherical than bubbles generated in the same liquid in normal gravity. This condition resulted in the pressure force dominating bubble dynamics for this liquid at low subcooling in zero gravity and at high subcooling for both gravity levels. Since the maximum distortion of a bubble occurs during collapse, the ethanol-water bubbles may be more spherical because of their characteristic proportionately longer growth times (fig. 10).

In summary, there was little change in the average maximum radius and lifetime of bubbles in a boiling ethanol-water solution when the gravity level was essentially removed. This condition is attributed, at high subcooling, to the dominance of the pressure force in both normal and zero gravity and, at low subcooling, to the increased importance of the pressure force in zero gravity as compared with normal gravity. The predominance of the pressure force is caused by the spherical shape of the bubbles.

SUMMARY OF RESULTS

An experimental and analytical study of the effect of an increase in viscosity in comparison with the viscosity of water, on the dynamics of vapor bubbles generated on a flat surface yielded the following results for a sucrose solution:

1. During the growth phase, the viscous effects on bubbles in the direction perpendicular to the heater surface are negligible.

2. The drag force is of consequence near separation for bubbles generated in a relatively viscous fluid in zero gravity.

A similar study of the effect of a reduction in surface tension in comparison with that for water indicated the following results for an ethanol-water solution:

3. At a particular subcooling, the average-lifetime and maximum-radii characteristics of bubbles were similar in normal and zero gravities.

4. The dimensionless growth times were longer than for comparable test conditions in water.

5. There was no necking down of the bubbles, and their contact angles remained relatively small at separation.

6. The bubbles remained more spherical than those in water, resulting in a greater pressure force over a longer portion of the lifetime. Consequently, at high subcooling in both gravity levels and at low subcooling in zero gravity, the pressure force dominated bubble removal.

Lewis Research Center,
National Aeronautics and Space Administration,
Cleveland, Ohio, April 5, 1967,
124-09-03-01-22.

APPENDIX A

SYMBOLS

D	diameter, ft; m
F_B	buoyancy force, lb force; N
F_{dr}	drag force, lb force; N
F_{dy}	dynamic force, lb force; N
F_P	pressure force, lb force; N
F_{sy}	surface-tension force, lb force; N
g	acceleration due to gravity, ft/sec ² ; m/sec ²
g_c	gravitational constant, lb mass/(lb force)(ft/sec ²); kg/(N)(m/sec ²)
K	constant peculiar to each liquid
P	pressure, lb force/sq ft; N/sq m
R	radius measured from bubble center of mass, ft; m
R_t	radius of curvature of top surface, ft; m
r	radius measured from nucleation site, ft; m
T	temperature, °F; °C
t	time, sec
V	bubble total volume, cu ft; cu m
V_b	bubble volume directly over base, cu ft; cu m
v	velocity, ft/sec; m/sec
v_r	velocity in r-direction, ft/sec; m/sec
v_θ	velocity in θ -direction, ft/sec; m/sec
y	distance above heater surface to bubble center of mass, ft; m
θ	angular displacement of r, rad
μ	dynamic viscosity, (lb force)/(sec)(sq ft); N/(sec)(sq m)
ρ	density, lb mass/cu ft; kg/cu m
σ	surface tension, lb force/ft; N/m
τ	dimensionless time

φ contact angle

Subscripts:

b base

l liquid

max maximum

S heater surface

sat saturated conditions

v vapor

w water

APPENDIX B

SURFACE-TENSION FORMULATION

The surface tension of water as a function of temperature was determined from

$$\sigma_w = 51.8 \times 10^{-4} \left(1 - \frac{T}{694.4} \right)^{1.2} \quad (B1)$$

as presented in reference 11. The relation between the surface tension of water and some other aqueous organic solution is presented in reference 12 as

$$\frac{\sigma}{\sigma_w} = 1 - K \quad (B2)$$

where K is a constant peculiar to each liquid. Inserting equation (B1) into equation (B2) and solving for σ results in

$$\sigma = (1 - K) (51.8 \times 10^{-4}) \left(1 - \frac{T}{694.4} \right)^{1.2} \quad (B3)$$

The constant K is determined from equation (B3) by inserting a known value of σ at some temperature. The known value of σ for the ethanol-water solution was taken directly from reference 6, and for the sucrose solution it was obtained by extrapolating data from that reference. The approximations obtained from this formulation are considered to be reasonably accurate because the liquids were far from their respective critical points.

REFERENCES

1. Aydelott, John C.: Self Pressurization of Liquid Hydrogen Tankage. M.S. Thesis, Cornell University, 1967.
2. Cochran, Thomas H.; and Aydelott, John C.: Effects of Subcooling and Gravity Level on Boiling in the Discrete Bubble Region. NASA TN D-3449, 1966.
3. Gaertner, R. F.: Photographic Study of Nucleate Pool Boiling on a Horizontal Surface. J. Heat Trans., vol. 87, no. 1, Feb. 1965, pp. 17-29.
4. Swindells, J. F.; Snyder, C. F.; Hardy, R. C.; and Golden, P. E.: Viscosities of Sucrose Solutions at Various Temperatures: Tables of Recalculated Values. Circular 440, supplement, National Bureau of Standards, July 31, 1958.
5. Kreith, Frank: Principles of Heat Transfer. Second ed., International Textbook Co., 1965.
6. Weast, Robert C., ed.: Handbook of Chemistry and Physics. 46th ed., Chemical Rubber Co., Cleveland, 1965.
7. Gray, Dwight E., ed.: American Institute of Physics Handbook. McGraw-Hill Book Co., Inc., 1957.
8. Weast, Robert C., ed.: Handbook of Chemistry and Physics. 44th ed., Chemical Rubber Co., Cleveland, 1963.
9. Keshock, Edward G.; and Siegel, Robert: Forces Acting on Bubbles in Nucleate Boiling Under Normal and Reduced Gravity Conditions. NASA TN D-2299, 1964.
10. Siegel, Robert: Effects of Reduced Gravity on Heat Transfer. Advances in Heat Transfer. Vol. 4, Thomas F. Irvine, Jr. and James P. Hartnett, eds., Academic Press, 1967, pp.
11. Zemansky, Mark W.: Heat and Thermodynamics. McGraw-Hill Book Co., Inc., 1957, p. 291.
12. Adamson, Arthur W.: Physical Chemistry of Surfaces. Interscience Publishers, Inc., 1960, p. 71.

TABLE I. - HEAT-TRANSFER DATA FOR BOILING FROM A HORIZONTAL FLAT SURFACE

Liquid	Heat flux		Subcooling		Average surface temperature		Gravity, g
	Btu/(hr)(sq ft)	W/sq m	°F	°C	°F	°C	
Sucrose	44 200	139 000	6.5	3.62	256	124.5	1
			15	8.34	254.5	123.5	1
			22.5	12.50	252.75	122.5	1
			6.5	3.62	-----	-----	0
			15.75	9.00	-----	-----	0
			22	12.22	-----	-----	0
Ethanol-water solution	44 200	139 000	4.5	2.50	221	105	1
	44 200	139 000	12.25	7.00	219.5	104	1
	44 200	139 000	21	11.67	217.75	103.25	1
	45 600	144 000	6	3.34	-----	-----	0
	45 600	144 000	14	7.78	-----	-----	0
	45 600	144 000	21	11.67	-----	-----	0

TABLE II. - COMPARISON OF MAGNITUDE OF VISCOUS AND LIQUID INERTIA TERMS

FROM EQUATION OF MOTION (EQ. (10))

Angular displace- ment of r, θ , deg	Time, t, sec	Liquid inertia terms				Viscous term, $\frac{\mu_L}{r^2} \frac{\partial^2 v_r}{\partial \theta^2}$	
		$\rho_L (\partial v_r / \partial t)$		$\rho_L v_r (\partial v_r / \partial r)$			
		lb mass	kg	lb mass	kg		
		(sq ft)(sec ²)	(sq m)(sec ²)	(sq ft)(sec ²)	(sq m)(sec ²)	lb mass (sq ft)(sec ²)	kg (sq m)(sec ²)
10	19×10^{-5}	-1.23×10^5	-6.00×10^5	-1.24×10^5	-6.05×10^5	-1.86×10^1	-9.07×10^1
	380	-3.68×10^4	-17.96×10^4	-3.57×10^4	-17.42×10^4	-6.91×10^{-2}	-33.72×10^{-2}
	605	-1.13×10^4	-5.51×10^4	-1.79×10^4	-8.73×10^4	-2.01×10^{-2}	-9.81×10^{-2}
30	19×10^{-5}	-2.85×10^5	-13.91×10^5	-9.95×10^4	-48.6×10^4	-6.35	-30.99
	380	-2.51×10^4	-12.25×10^4	-2.76×10^4	-13.47×10^4	-2.86×10^{-2}	-13.96×10^{-2}
	665	-6.50×10^3	-31.72×10^3	-7.49×10^3	-36.55×10^3	-1.38×10^{-2}	-6.73×10^{-2}
60	19×10^{-5}	-1.71×10^5	8.34×10^5	-9.18×10^4	-44.80×10^4	2.24	10.93
	380	-1.57×10^4	7.66×10^4	-1.23×10^4	-6.00×10^4	2.5×10^{-4}	12.20×10^{-4}
	665	-4.87×10^3	23.76×10^3	-5.79×10^3	-2.82×10^3	-1.64×10^{-2}	-8.0×10^{-2}
90	19×10^{-5}	-2.04×10^5	-9.96×10^5	-1.5×10^5	-7.3×10^5	9.89	48.26
	380	-1.08×10^4	-5.27×10^4	-1.46×10^4	7.12×10^4	2.61×10^{-2}	12.74×10^{-2}
	665	-9.72×10^3	-47.4×10^3	-6.18×10^3	-30.16×10^3	-1.79×10^{-2}	-8.74×10^{-2}

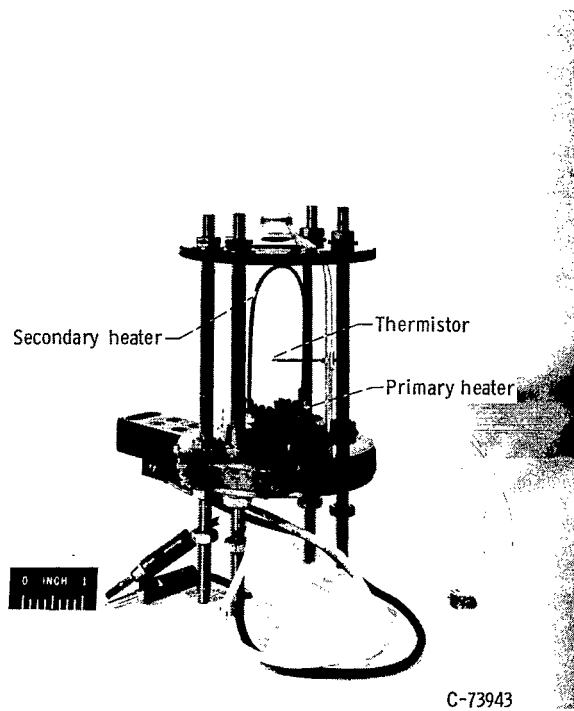


Figure 1. - Boiler apparatus.

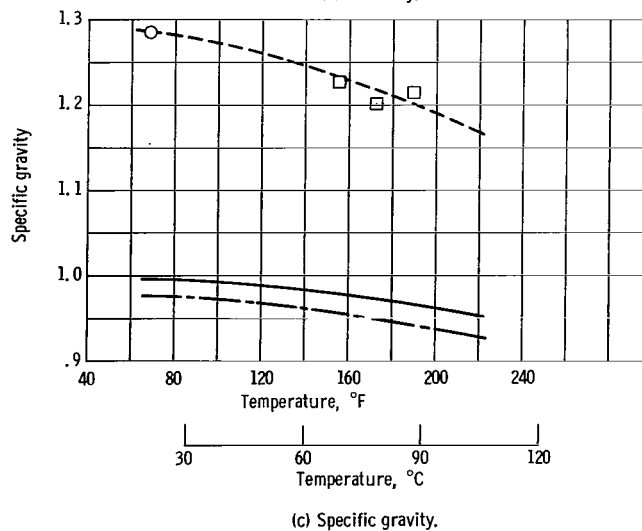
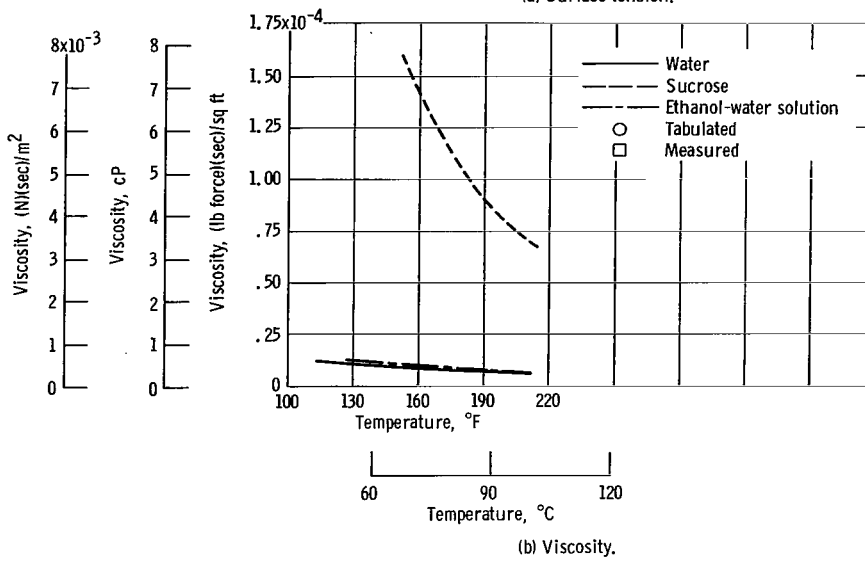
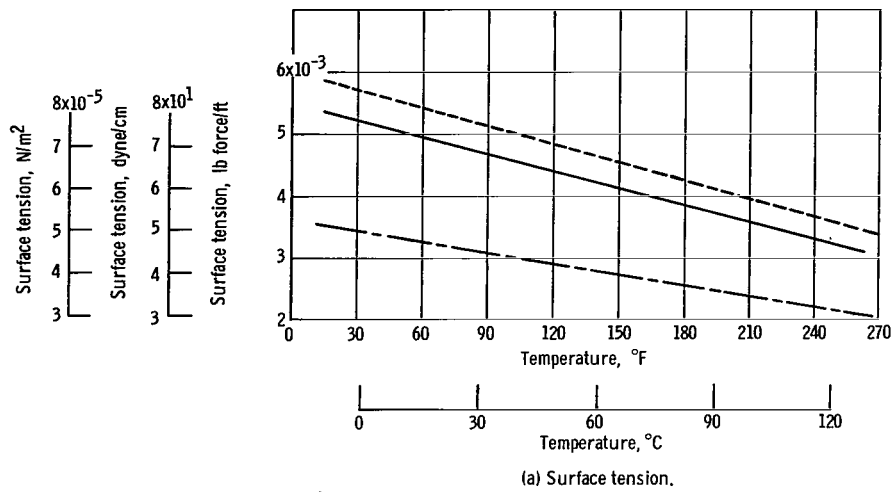
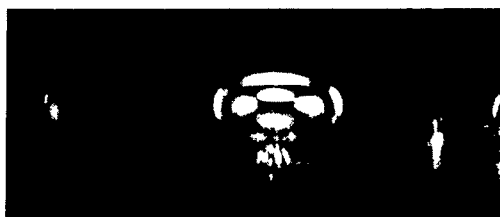


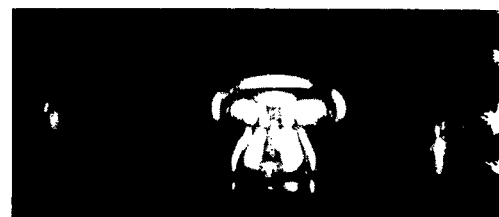
Figure 2. - Effect of temperature on surface tension, viscosity, and specific gravity.



(a)



(b)



(c)



(d)



(e)



(f)



(g)



(h)

C-67-1489

Figure 3. - Coalescence of successive bubbles in sucrose solution.

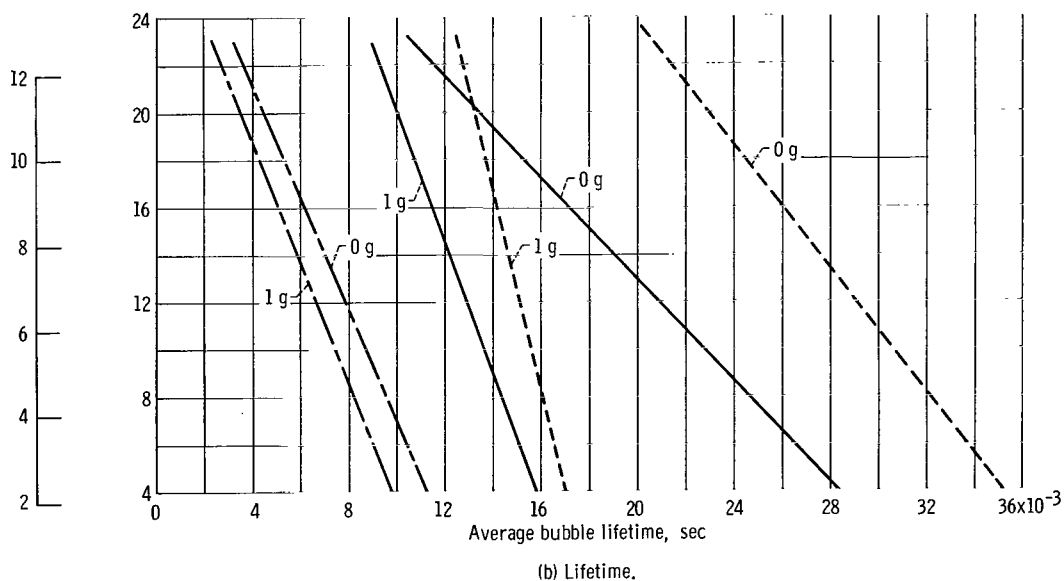
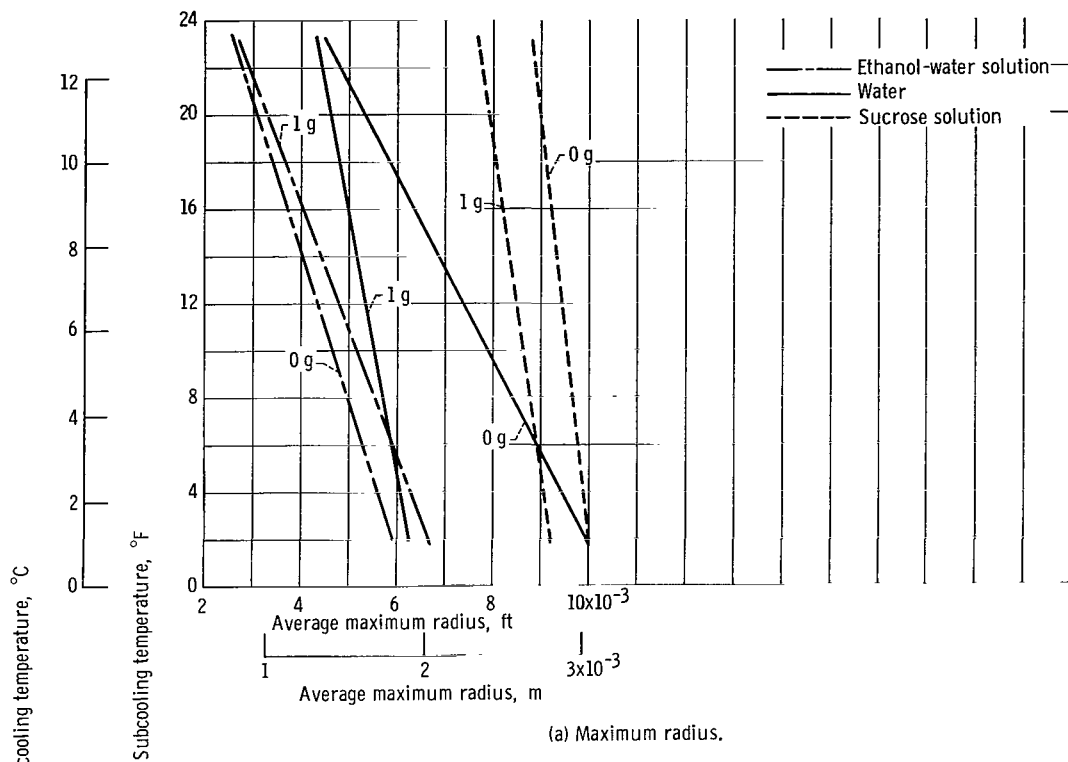
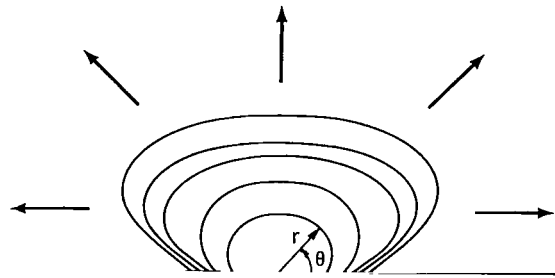
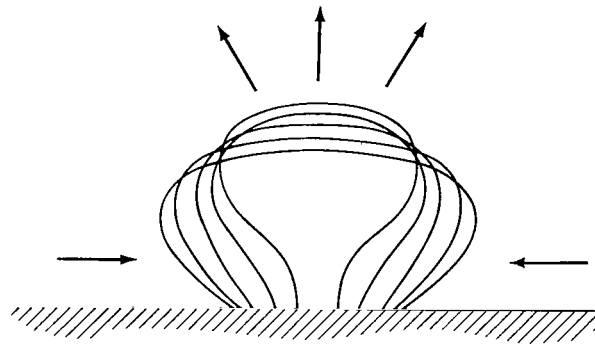


Figure 4. - Effect of subcooling and fluid properties on bubble maximum radius and lifetime.

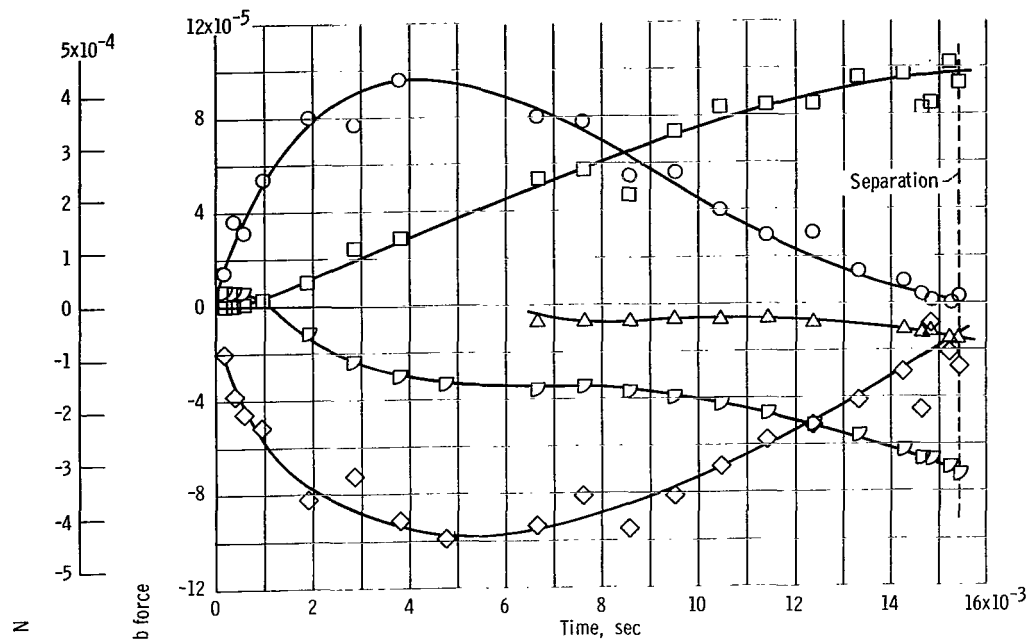


(a) Bubble growth.

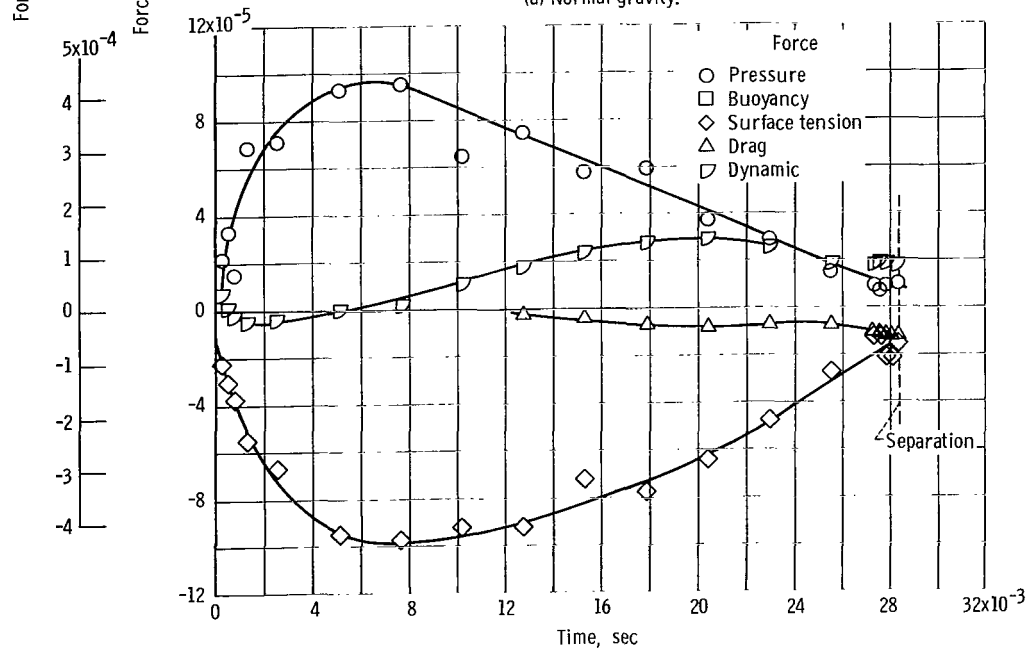


(b) Bubble collapse.

Figure 5. - Profiles of bubble at 22.9° F (12.8° C) subcooling and zero gravity illustrating liquid flow patterns.



(a) Normal gravity.



(b) Zero gravity.

Figure 6. - Dynamics of sucrose bubble at approximately 15° F (8.34° C) subcooling in normal and zero gravity.

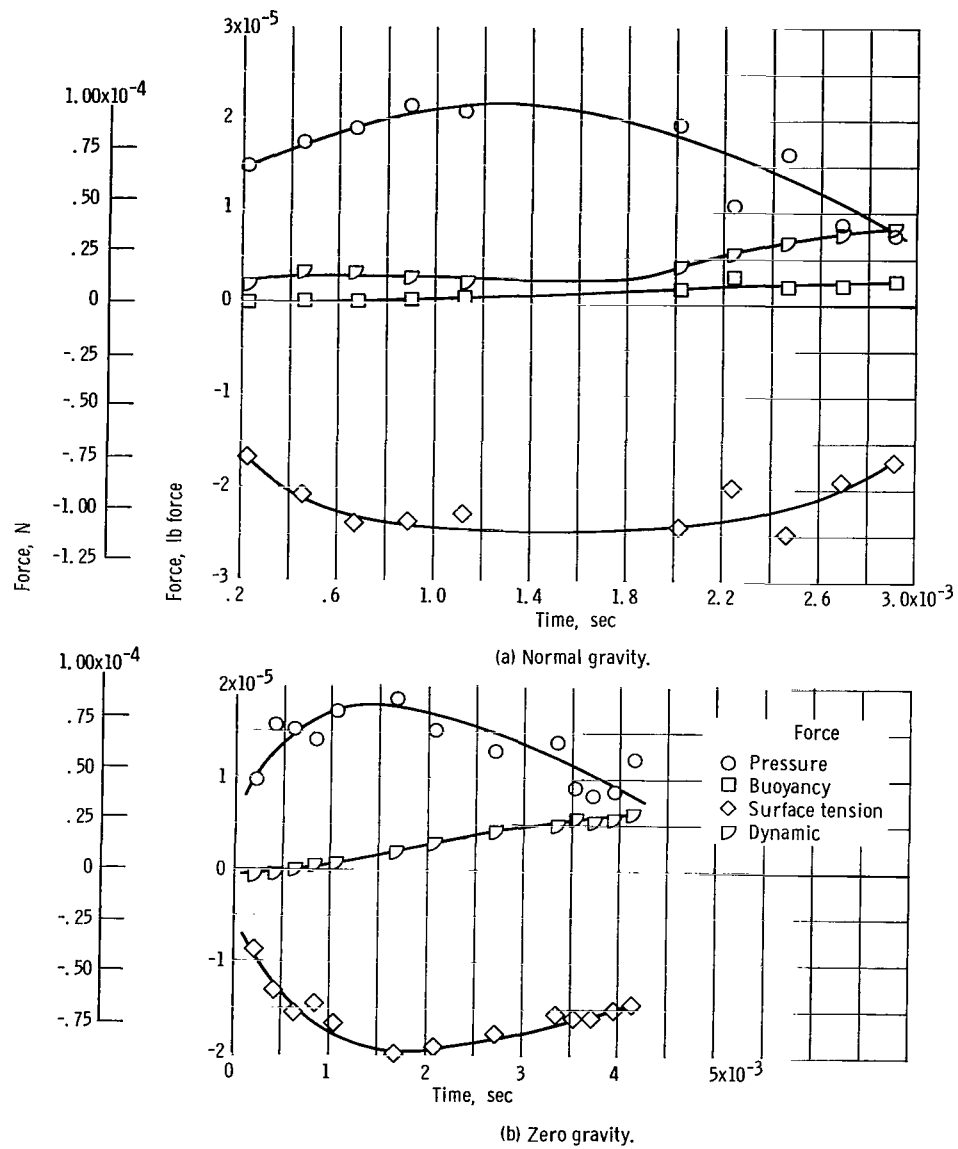


Figure 7. - Dynamics of ethanol-water bubble at approximately 21° F (11.67° C) subcooling in normal and zero gravity.

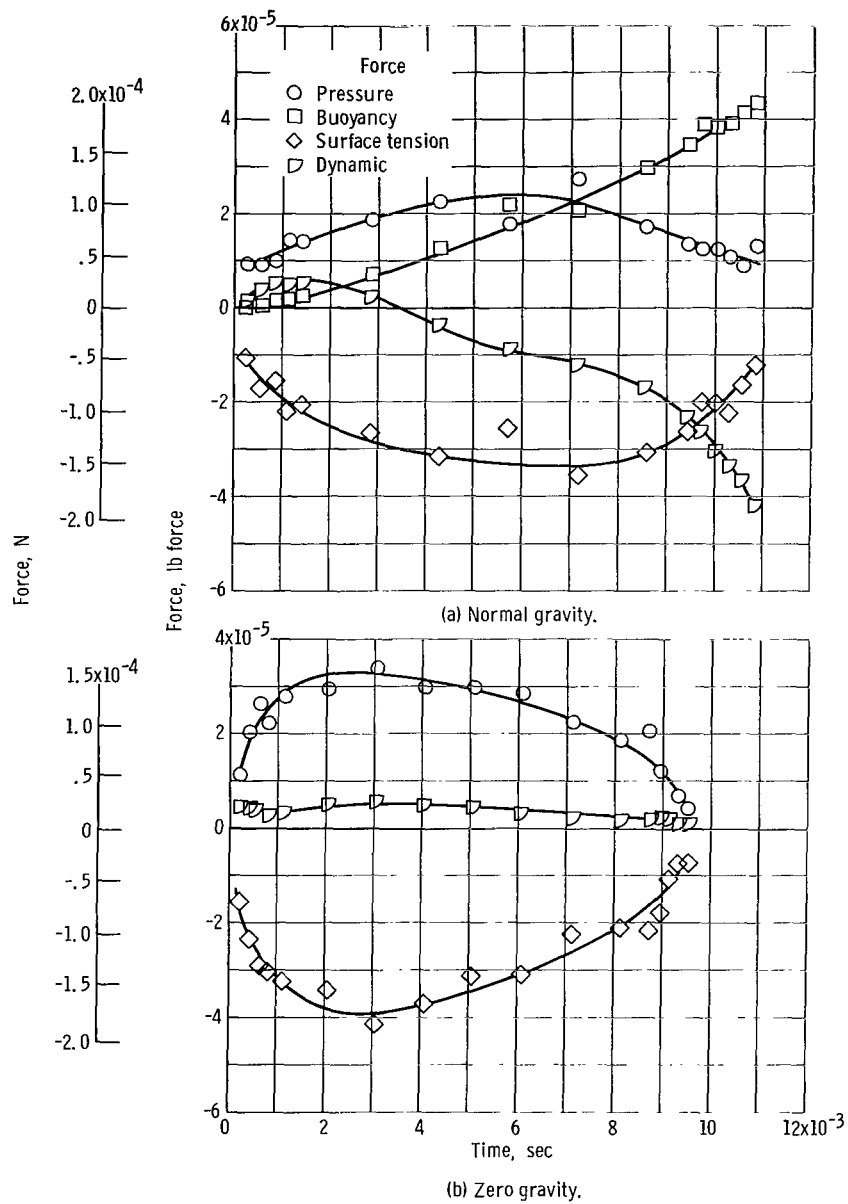


Figure 8. - Dynamics of ethanol-water bubble at approximately 5° F (2.78° C) subcooling in normal and zero gravity.

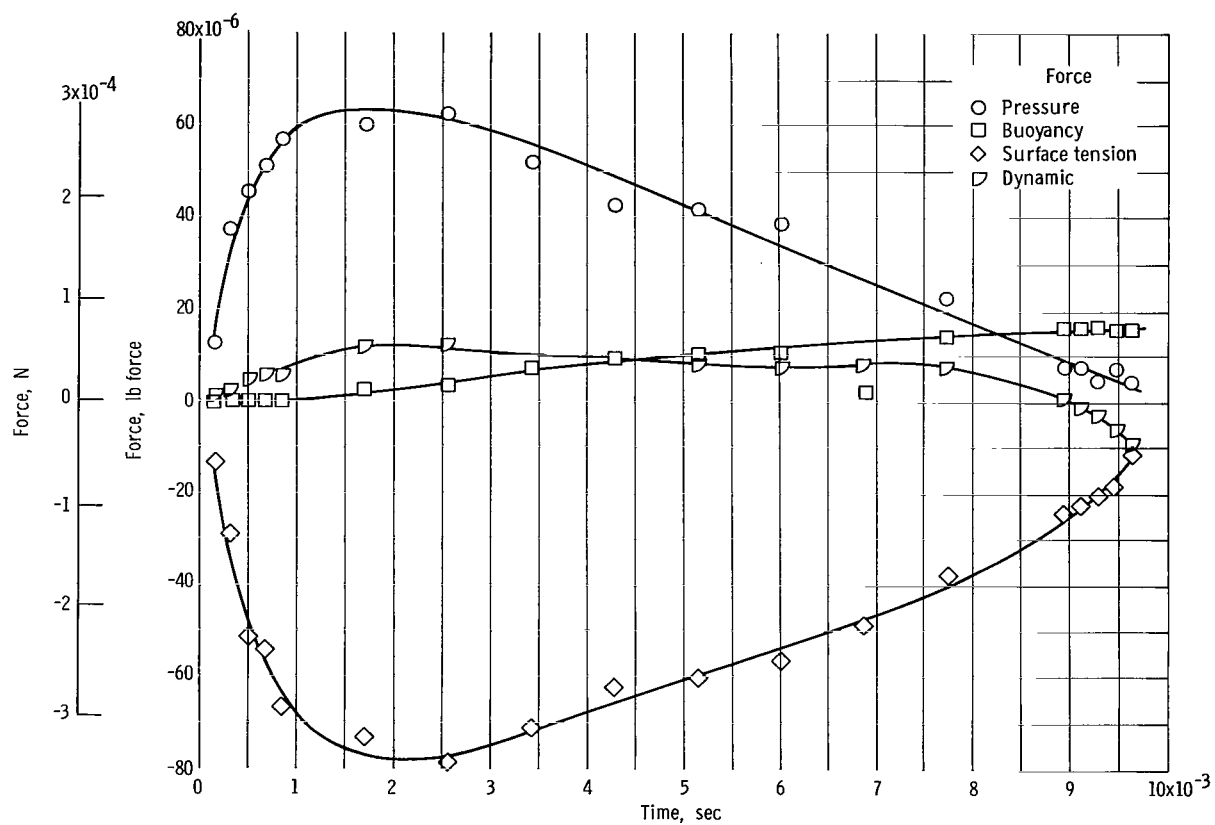


Figure 9. - Dynamics of water bubble at approximately 14.1° F (7.8° C) subcooling and normal gravity.

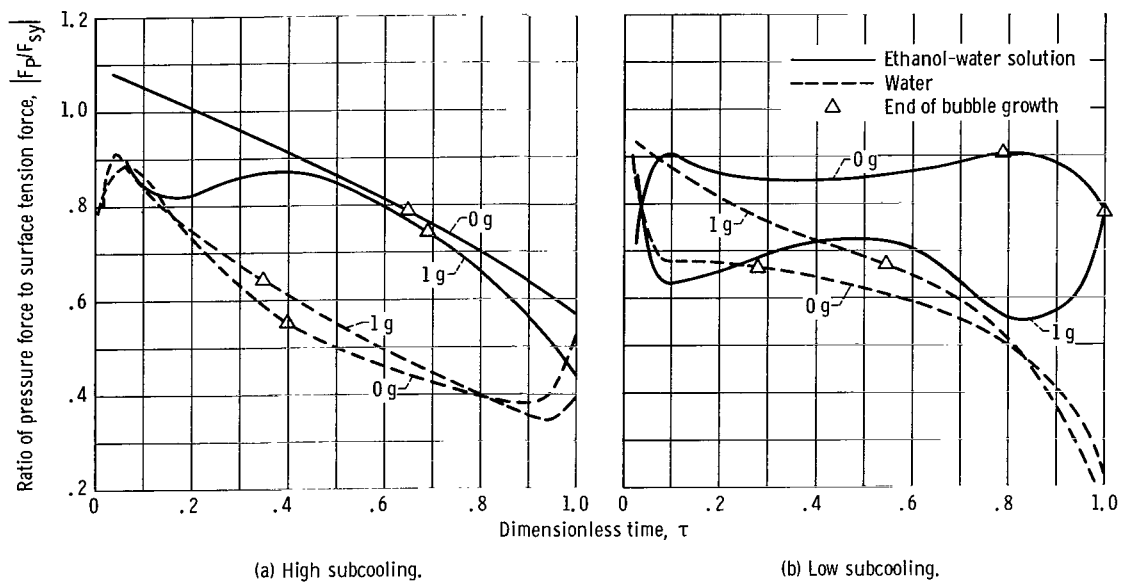


Figure 10. - Distortion of bubbles from spherical shape at high and low subcooling.

"The aeronautical and space activities of the United States shall be conducted so as to contribute . . . to the expansion of human knowledge of phenomena in the atmosphere and space. The Administration shall provide for the widest practicable and appropriate dissemination of information concerning its activities and the results thereof."

—NATIONAL AERONAUTICS AND SPACE ACT OF 1958

NASA SCIENTIFIC AND TECHNICAL PUBLICATIONS

TECHNICAL REPORTS: Scientific and technical information considered important, complete, and a lasting contribution to existing knowledge.

TECHNICAL NOTES: Information less broad in scope but nevertheless of importance as a contribution to existing knowledge.

TECHNICAL MEMORANDUMS: Information receiving limited distribution because of preliminary data, security classification, or other reasons.

CONTRACTOR REPORTS: Scientific and technical information generated under a NASA contract or grant and considered an important contribution to existing knowledge.

TECHNICAL TRANSLATIONS: Information published in a foreign language considered to merit NASA distribution in English.

SPECIAL PUBLICATIONS: Information derived from or of value to NASA activities. Publications include conference proceedings, monographs, data compilations, handbooks, sourcebooks, and special bibliographies.

TECHNOLOGY UTILIZATION PUBLICATIONS: Information on technology used by NASA that may be of particular interest in commercial and other non-aerospace applications. Publications include Tech Briefs, Technology Utilization Reports and Notes, and Technology Surveys.

Details on the availability of these publications may be obtained from:

SCIENTIFIC AND TECHNICAL INFORMATION DIVISION
NATIONAL AERONAUTICS AND SPACE ADMINISTRATION
Washington, D.C. 20546